membrane was rehybridized with a *β-actin* probe. (d) Western blot analysis of MDA5 expression. WT and MDA5$^{-/-}$ MEFs were treated with 1000 U/ml IFN-β for 8 h, and whole cell lysates were immunoblotted with antibody against MDA5. N.S. non specific.

Supplementary Fig. 2. Involvement of MDA5 or RIG-I in the recognition of dsRNAs.

(a) RIG-I$^{-/-}$ and MDA5$^{-/-}$, and their littermate WT mice were injected intravenously with 200 μg of poly I:C for the indicated periods and the production of IFN-β in the sera was measured by ELISA. The data are means ± S.D. of sera samples.

(b) GMCSF-DCs from RIG-I$^{-/-}$ and MDA5$^{-/-}$, TRIF$^{-/-}$ and their littermate control mice were incubated in the presence of 50, 250 μg/ml poly I:C for 24 h. The production of IFN-α in the culture supernatants was measured by ELISA.

(c) Generation of different lengths of dsRNAs corresponding to mouse lamin A/C. Different lengths of dsRNAs corresponding to mouse lamin A/C were synthesized as described in Methods section. 1 μg of dsRNAs were separated on 1% Agarose gel and visualized by staining with ethidium bromide. All dsRNAs synthesized appear with the estimated size.

Supplementary Fig. 3: Contribution of RIG-I and MDA5 in the induction of genes encoding type I IFNs and IFN-inducible proteins in response to viral infection.

(a) WT, RIG-I$^{-/-}$ or MDA5$^{-/-}$ MEFs were treated with 5 μg/ml poly I:C complexed with lipofectamine 2000 for the indicated periods. Total RNA was extracted and subjected to the Northern blot analysis for the expression of *IFN-β*, *IP10* and *β-actin* mRNA.

(b) WT, RIG-I$^{-/-}$ and MDA5$^{-/-}$ MEFs were treated with 5 μg/ml dsRNA corresponding to Lamin A/C (600 bps) complexed with lipofectamine 2000 for the indicated periods. Total RNA was extracted and subjected to the Northern blot analysis for the expression of

IFN-β and *IP10* mRNA. 28S and 18S ribosomal RNA bands on ethidium bromide-stained gel were used to control the RNA loading (lower panel).

(c) WT, RIG-I$^{-/-}$ and MDA5$^{-/-}$ MEFs were infected with moi=10 of SeV V(-) for the indicated periods. Total RNA was extracted and subjected to the Northern blot analysis for the expression of *IFN-β* and *IP10* mRNA. 28S and 18S ribosomal RNA bands on ethidium bromide-stained gel were used to control the RNA loading (lower panel).

(d) WT and MDA5$^{-/-}$ PECs were exposed to moi=10 of EMCV for the indicated periods. Total RNA was extracted and subjected to the Northern blot analysis for the expression of *IFN-β*, *IP10*, *IL-6* and *β-actin* mRNA.

Supplementary Fig. 4: Role of MDA5 and RIG-I in the IFN-α responses against various viruses.

(a) WT, RIG-I$^{-/-}$ and MDA5$^{-/-}$ MEFs were exposed to negative-sense ssRNA viruses, including NDV, VSV NCP, SeV Cm, SeV V- and influenza ΔNS1. IFN-α production in the culture supernatants was measured by ELISA.

(b and c) GMCSF-DCs from RIG-I$^{-/-}$ and MDA5$^{-/-}$ mice and their littermate WT mice were infected with indicated moi of EMCV for 24 h. The production of IFN-α (b) and IL-6 (c) in the culture supernatants was measured by ELISA.

(d) GMCSF-DCs from wild-type and MDA5$^{-/-}$ mice were infected with indicated moi of Theiler's virus or Mengovirus for 24 h. IFN-α production in the culture supernatants was measured by ELISA. The data are means ± S.D. of tripricates.

Supplementary Fig. 5: EMCV-mediated protein synthesis shutoff was not altered between wild-type and MDA5$^{-/-}$ MEFs.

Cultures of wild-type and MDA5$^{-/-}$ MEFs were infected with EMCV and labeled by incorporation of [^{35}S]Met-Cys for 1 h at various times after infection. Total cell extracts

were separated by polyacrylamide gel electrophoresis, and the proteins were visualized by autoradiography.

Supplementary Fig. 6: Differential involvement of MDA5 and MyD88 in EMCV-mediated IFN production in cDCs and pDCs.

DCs were induced from bone marrow cells obtained from MyD88$^{+/-}$, MyD88$^{-/-}$, MDA5$^{+/-}$ and MDA5$^{-/-}$ mice by cultivating in the presence of Flt3L. At day 7, B220^{+}CD11c^{+} pDCs and B220^{-}CD11c^{+} cDCs were purified by MACS, and infected with EMCV for 24h. IFN-α production in the culture supernatants was measured by ELISA. Error bars indicate ± S.D. of triplicates.

Supplementary Fig. 7: The survival of MDA5$^{-/-}$, RIG-I$^{-/-}$ or IFNα/βR$^{-/-}$ mice in response to VSV infection.

The survival of the mice (3-weeks old) infected with $4x10^6$ pfu VSV intranasally was monitored for 9 days ($p<0.01$ by the generalized wilcoxon test between RIG-I$^{-/-}$ mice and their littermate controls).

Supplementary Fig. 8: Responses of MDA5$^{-/-}$ mice against EMCV infection

(a) MDA5$^{+/-}$ and MDA5$^{-/-}$ mice (n=5) were intravenously inoculated with 1 X 10^7 pfu EMCV. Sera were taken at 4 h after injection, and IFN-β, Rantes and IL-6 production levels were determined by ELISA. *, $P<0.05$ versus controls by the student's t-test.

(b) Cardiac function of the mice 48 h after EMCV infection was assessed by echocardiography. Transthoracic M-mode echocardiographic tracings from MDA5$^{+/-}$ and MDA5$^{-/-}$ mice 48 h after EMCV infection.

Supplementary Table I: Genotypes of mice derived from RIG-I$^{+/-}$ intercrosses or crosses between RIG-I$^{+/-}$ and RIG-I$^{-/-}$ mice.

Supplemental Figure 1.

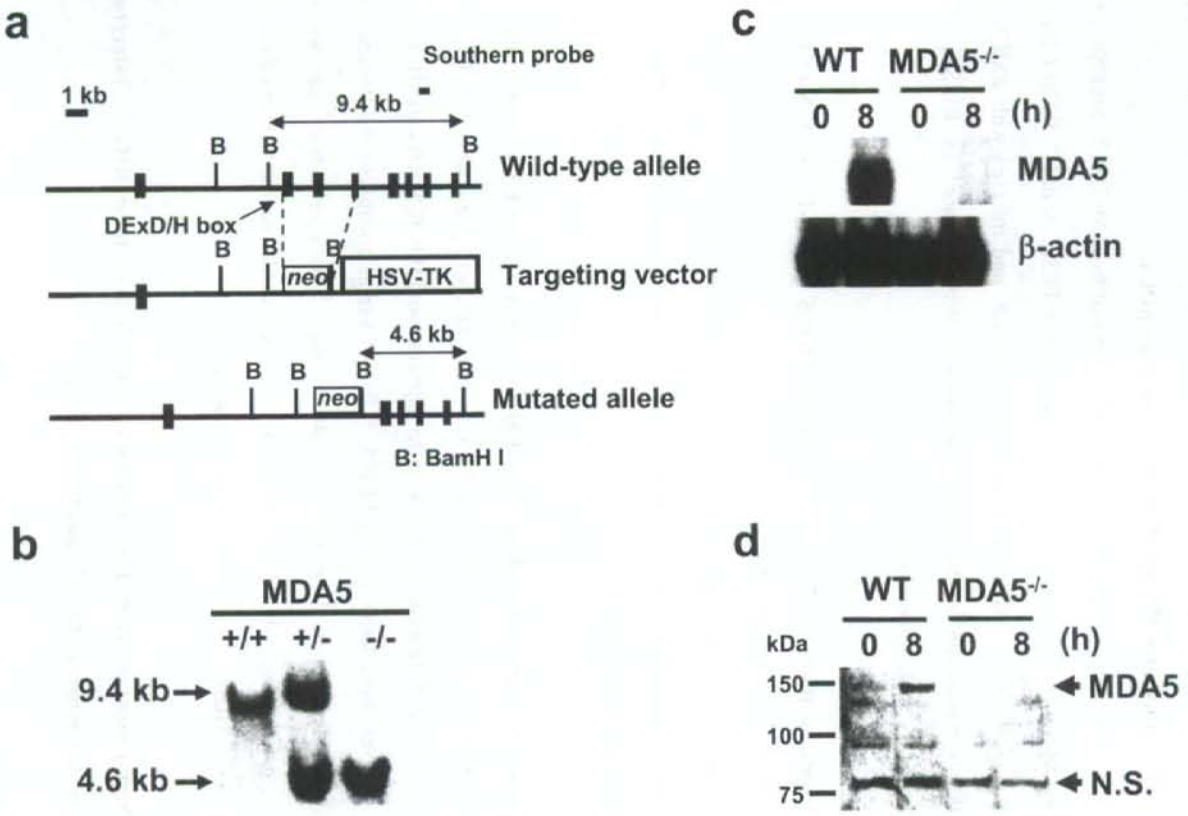

Supplemental Figure 2.

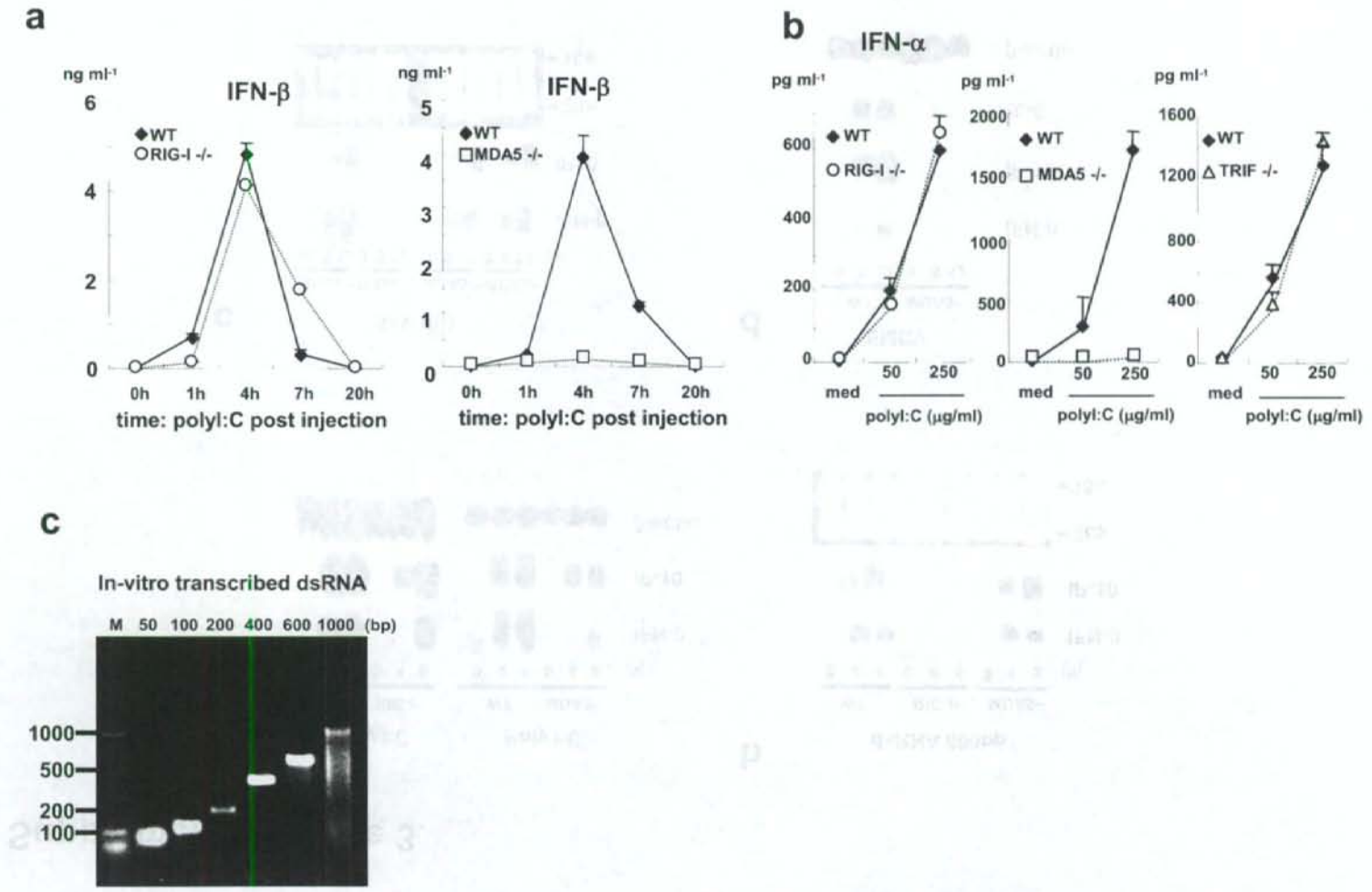

Supplemental Figure 3.

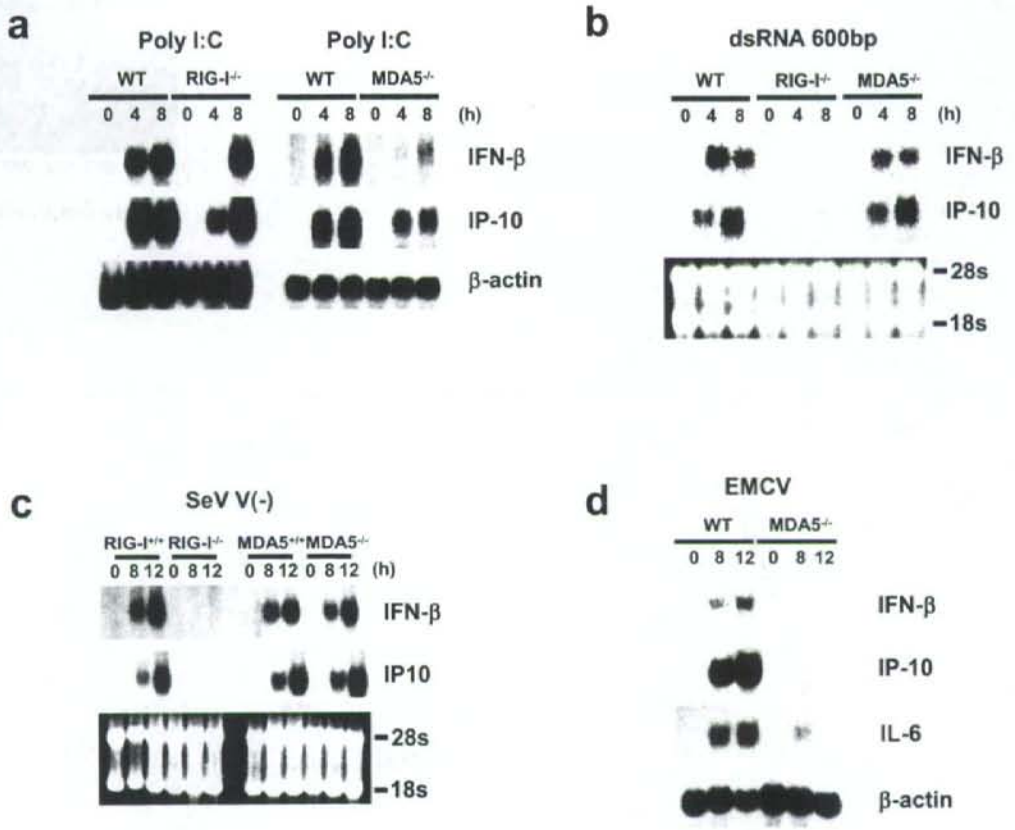

Supplemental Figure 4.

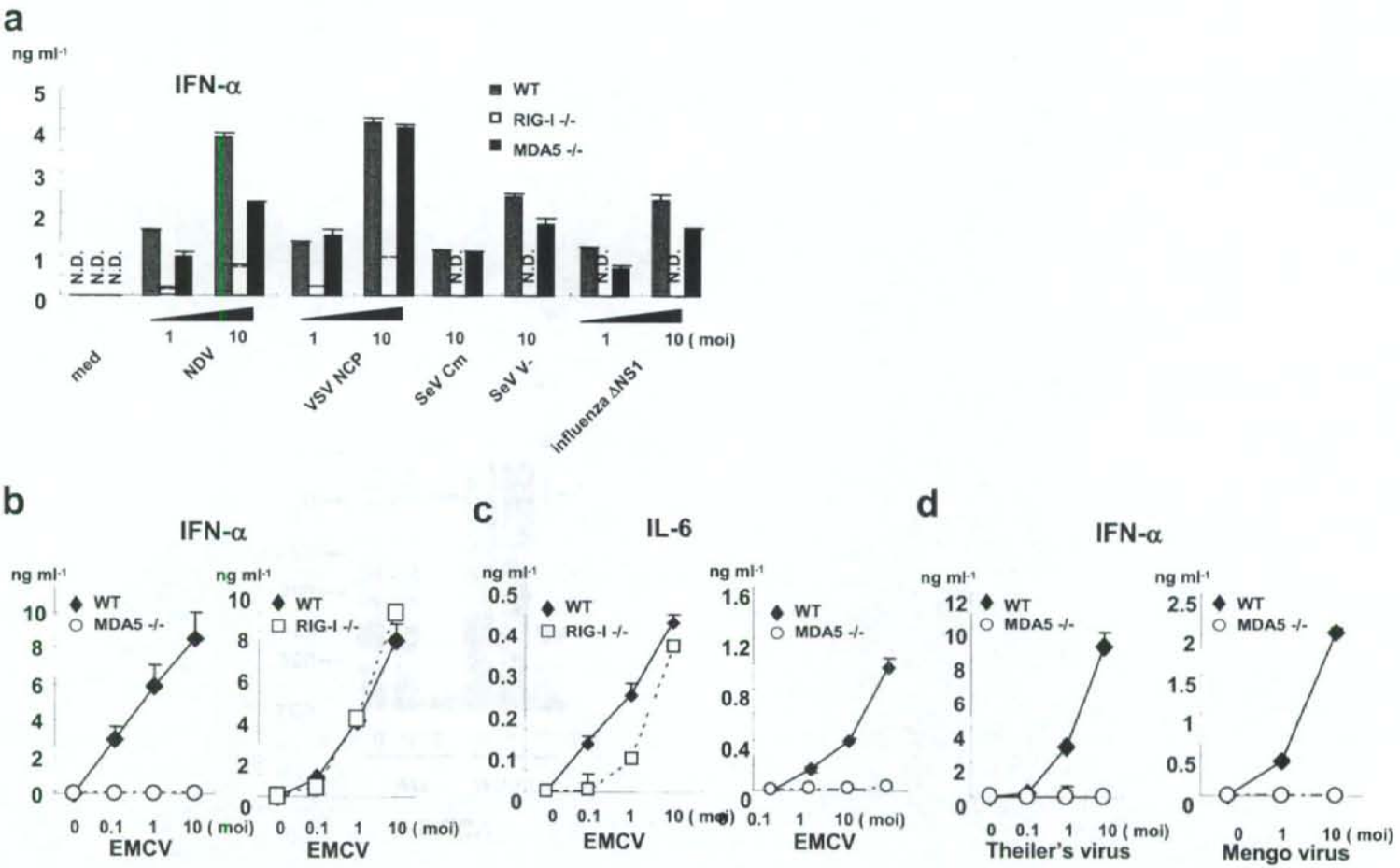

Supplemental Figure 5.

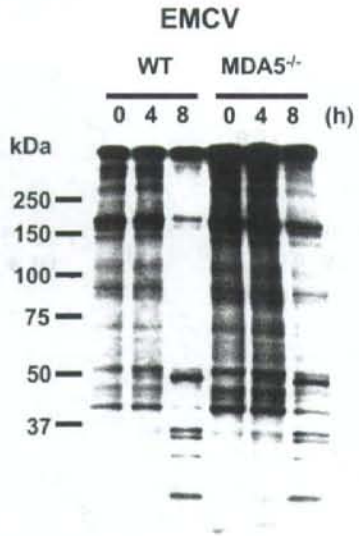

Supplemental Figure 6.

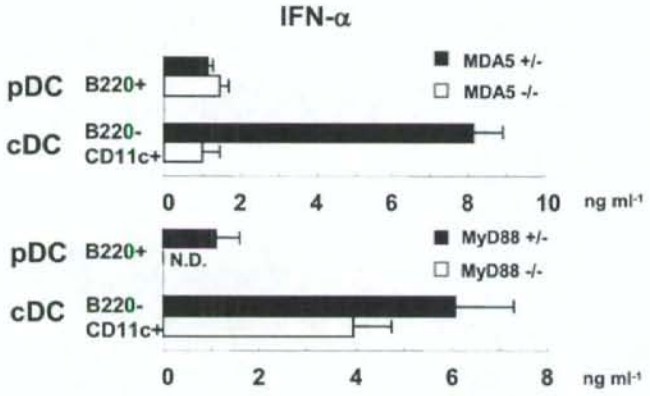

Supplemental Figure 7.

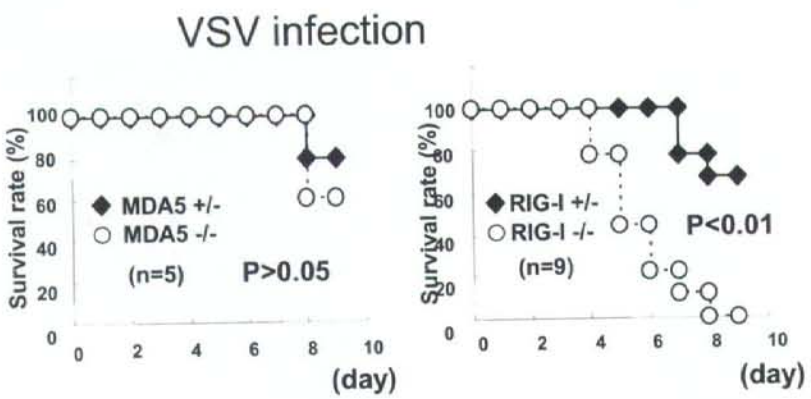

Supplemental Figure 8.

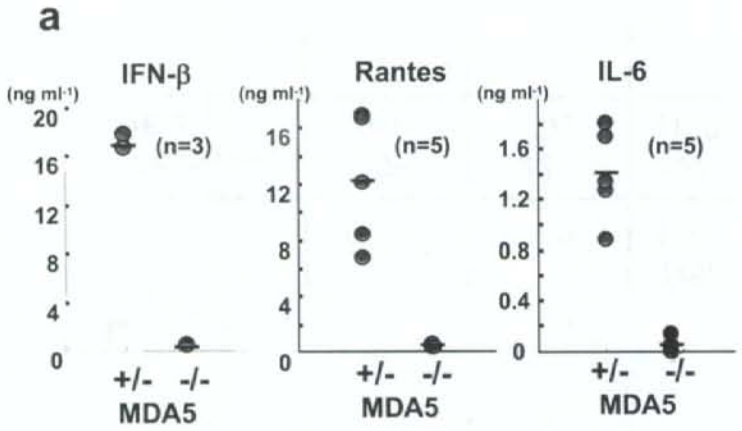

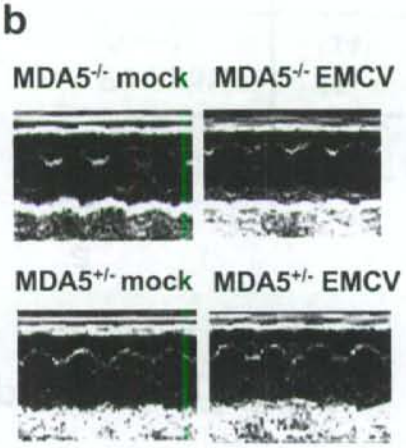

Supplemental Table 1.

a

	RIG-I$^{+/+}$	RIG-I$^{+/-}$	RIG-I$^{-/-}$	Total (%)
Postnatal (6w~)	16 (34)	28 (60)	3 (6)	47 (100)

b

	RIG-I$^{+/-}$	RIG-I$^{-/-}$	Total (%)
Postnatal (6w~)	108 (83)	22 (17)	130 (100)

Available online at www.sciencedirect.com
SCIENCE DIRECT
VIROLOGY
Virology 351 (2006) 381–392
www.elsevier.com/locate/yviro

Production of infectious hepatitis C virus particles in three-dimensional cultures of the cell line carrying the genome-length dicistronic viral RNA of genotype 1b

Kyoko Murakami [a], Koji Ishii [a], Yousuke Ishihara [b], Sayaka Yoshizaki [a], Keiko Tanaka [c], Yasufumi Gotoh [d,e], Hideki Aizaki [a], Michinori Kohara [f], Hiroshi Yoshioka [g], Yuichi Mori [g], Noboru Manabe [d], Ikuo Shoji [a], Tetsutaro Sata [c], Ralf Bartenschlager [h], Yoshiharu Matsuura [i], Tatsuo Miyamura [a], Tetsuro Suzuki [a,*]

[a] *Department of Virology II, National Institute of Infectious Diseases, 1-23-1 Toyama, Shinjuku-ku, Tokyo 162-8640, Japan*
[b] *Hanaichi Ultrastructure Research Institute, Okazaki, Aichi 444-0076, Japan*
[c] *Department of Pathology, National Institute of Infectious Diseases, Shinjuku, Tokyo 162-8640, Japan*
[d] *Research Unit for Animal Life Sciences, Animal Resource Science Center, The University of Tokyo, Iwama, Ibaraki 319-0206, Japan*
[e] *Unit of Anatomy and Cell Biology, Department of Animal Sciences, Kyoto University, Kyoto 606-8502, Japan*
[f] *Department of Microbiology and Cell Biology, Tokyo Metropolitan Institute of Medical Science, Bunkyo-ku, Tokyo 113-8613, Japan*
[g] *Mebiol Inc., Hiratsuka, Kanagawa 254-0075, Japan*
[h] *Department of Molecular Virology, Hygiene Institute, University Heidelberg, Im Neuenheimer Feld 345, D-69120 Heidelberg, Germany*
[i] *Department of Molecular Virology, Research Institute for Microbial Diseases, Osaka University, Suita, Osaka 565-0871, Japan*

Received 5 January 2006; returned to author with revision 23 January 2006; accepted 24 March 2006
Available online 6 May 2006

Abstract

We show that a dicistronic hepatitis C virus (HCV) genome of genotype 1b supports the production and secretion of infectious HCV particles in two independent three-dimensional (3D) culture systems, the radial-flow bioreactor and the thermoreversible gelation polymer (TGP), but not in monolayer cultures. Immunoreactive enveloped particles, which are 50–60 nm in diameter and are surrounded by membrane-like structures, are observed in the culture medium as well as at the endoplasmic reticulum membranes and in dilated cytoplasmic cisternae in spheroids of Huh-7 cells. Infection of HCV particles is neutralized by anti-E2 antibody or patient sera that interfere with E2 binding to human cells. Finally, the utility of the 3D-TGP culture system for the evaluation of antiviral drugs is shown. We conclude that the replicon-based 3D culture system allows the production of infectious HCV particles. This system is a valuable tool in studies of HCV morphogenesis in a natural host cell environment.

Keywords: Hepatitis C virus; Replication; Three-dimensional culture; Virus particle

Introduction

Infection with hepatitis C virus (HCV) currently represents a major medical and socioeconomic problem. HCV is a main causative agent of chronic hepatitis, cirrhosis, and hepatocellular carcinoma, and there are an estimated 170 million HCV carriers worldwide (Choo et al., 1989). The standard treatments for HCV infection are interferon alpha (IFN-α) in combination with ribavirin (RBV) or, more recently, a polyethylene glycol-modified form of IFN-α; however, sustained response is seen in only ~50% of treated patients (Davis et al., 2003; Manns et al., 2001). Further development of new anti-HCV drugs and vaccines has been obstructed by the lack of either a small animal model or a robust cell culture system capable of supporting viral replication and the production of infectious progeny.

HCV is a small enveloped RNA virus belonging to the family Flaviviridae and harboring a single-stranded RNA genome with

* Corresponding author. Fax: +81 3 5285 1161.
E-mail address: tesuzuki@nih.go.jp (T. Suzuki).

0042-6822/$ - see front matter © 2006 Elsevier Inc. All rights reserved.
doi:10.1016/j.virol.2006.03.038

positive polarity. A precursor polyprotein of ~3000 amino acids (aa) is encoded by a large open reading frame. This polyprotein is cleaved by cellular and viral proteases to give rise to a series of structural and nonstructural proteins (Choo et al., 1991; Grakoui et al., 1993; Hijikata et al., 1991). The establishment of selectable dicistronic HCV RNAs that are capable of autonomous replication in human hepatoma Huh-7 cells was a significant breakthrough in HCV research (Blight et al., 2000; Lohmann et al., 1999) and has provided an important tool for the study of HCV replication mechanisms and for screening antiviral drugs (Frese et al., 2001; Guo et al., 2001). This replicon system was first developed to replicate only viral subgenomic RNAs but has been further expanded to enable the replication of genome-length dicistronic RNAs (Ikeda et al., 2002; Pietschmann et al., 2002). Although the viral genome replicates and all HCV proteins are properly processed in this system, virus particle production has not yet been achieved. A number of researchers (Date et al., 2004; Kato et al., 2001, 2003) have developed an HCV genotype 2a replicon (JFH-1) that efficiently replicates in a variety of human cells. Recently, it has been demonstrated that the full-length JFH-1 genome or a chimeric genome using JFH-1 and J6, a related genotype 2a strain, produces infectious particles in cell cultures (Lindenbach et al., 2005; Wakita et al., 2005; Zhong et al., 2005). More recently, production of infectious genotype 1a virus (Hutchinson strain) using similar experimental systems has been described (Yi et al., 2006). These complete HCV culture systems produce robust levels of infectious virus and provides a powerful tool for HCV research. However, to date their applications have not been extended to constructs based on strains of genotype 1b, which is highly prevalent worldwide.

We previously demonstrated that differentiated human hepatoma FLC4 cells transfected with in vitro transcribed HCV genomic RNA can produce and secrete infectious particles in three-dimensional (3D) radial-flow bioreactor (RFB) culture (Aizaki et al., 2003). This RFB system was initially aimed to develop artificial liver tissue, and the bioreactor column consists of a vertically extended cylindrical matrix through which liquid medium flows continuously from the periphery toward the center of the reactor (Kawada et al., 1998). In RFB culture, human hepatocellular carcinoma-derived cells can grow spherically or cubically, and they retain liver functions such as albumin synthesis (Kawada et al., 1998; Matsuura et al., 1998) and drug-metabolizing activity mediated by cytochrome P450 3A4 (Iwahori et al., 2003).

In the present study, two kinds of 3D culture techniques, the RFB and the thermoreversible gelation polymer (TGP), were used for the production and secretion of infectious HCV particles by using a dicistronic HCV genome derived from genotype 1b. We also demonstrate that these 3D culture systems are useful for evaluating anti-HCV drugs.

Results

Secretion of HCV-LPs from RCYM1 carrying genome-length dicistronic HCV RNA cultured in RFB culture

We first assessed the replicative capacity of selectable genome-length HCV RNAs in FLC4 cells. However, no G418-resistant colonies were observed, indicating that FLC4 cells do not support replication of these HCV RNAs (data not shown). Therefore, subsequent experiments were carried out with a stable Huh-7 cell line, RCYM1, which supports full-length HCV RNA replication and which was developed by transfection of the cells with genome-length dicistronic RNA derived from the Con1 clone I389neo/core-3′/NK 5.1 (genotype 1b)

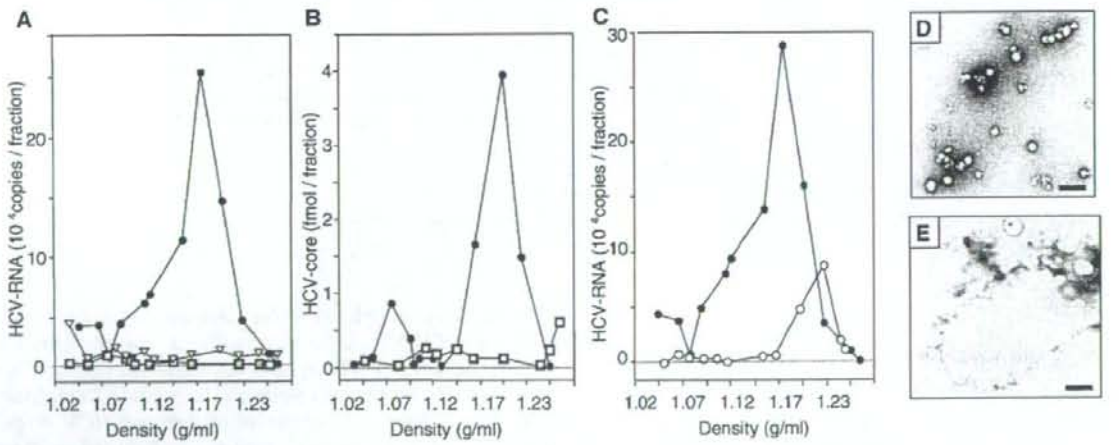

Fig. 1. Sucrose density gradient analysis of culture supernatants of RCYM1 cells. Culture media collected from radial-flow bioreactor (RFB)-cultured RCYM1 (closed circles), monolayer-cultured RCYM1 (open squares), and RFB-cultured 5–15 cells (open triangles) were fractionated as described in Materials and methods. (A) HCV RNA in each fraction was measured by real-time reverse transcriptase-polymerase chain reaction (RT-PCR). Mean values of duplicates were plotted against the density of the corresponding fraction. (B) HCV core protein in each fraction was determined by enzyme-linked immunosorbent assay (ELISA). Mean values of duplicates were plotted against the density. (C) Culture medium of RFB-cultured RCM1 cells were treated with 0.2% NP40 (open circles), followed by centrifugation in a sucrose gradient. Each fraction was tested for HCV RNA by real-time RT-PCR. (D, E) Electron microscopy analysis. Samples were prepared from the 1.18 g/ml fraction of culture media collected from RFB-cultured (D) or monolayer-cultured (E) RCYM1 cells.

(Pietschmann et al., 2002). The HCV RNA level in RCYM1 cells was approximately 5×10^6 copies/μg total RNA as determined by real-time reverse transcriptase-polymerase chain reaction (RT-PCR). The expression and subcellular localization of HCV protein were confirmed by Western blotting and immunofluorescence analysis (data not shown). To develop 3D RFB cultures, first we loaded RCYM1 cells onto an RFB column by flowing cell suspension, after which the cells were attached to carrier beads. Cells proliferated within the 3D matrix, and culture medium was circulated radially through the column.

In order to investigate whether HCV-like particles (HCV-LPs) were secreted from RCYM1 cells in the RFB culture system, we fractionated culture fluid collected after 5–10 days of culture by continuous 10–60% (wt/vol) sucrose density gradient centrifugation. HCV RNA and core protein were predominantly detected in the 1.15–1.20 g/ml fractions, with maximal detection in the 1.18 g/ml fraction (Figs. 1A and B). In the same experiment using 5–15 cells, in which a subgenomic HCV replicon replicates, no peak similar to that observed in RCYM1 cells corresponding to HCV RNA was detected. In both RCYM1 cells and 5–15 cells in the RFB culture system, a substantial amount of HCV RNA was detected in the 1.03–1.07 g/ml fractions (Fig. 1A). Consistent with a previous report by Pietschmann et al. (2002), these RNAs released from cells with a subgenomic replicon did not correspond to virus particles. When an equivalent number of RCYM1 cells were cultured in a monolayer culture system, limited amounts of HCV RNA and core protein were detected in the culture supernatant (Figs. 1A and B).

The mature HCV virion is thought to have a nucleocapsid and an outer envelope composed of a lipid membrane with viral envelope glycoproteins. Culture fluids were treated with NP40 in order to solubilize lipids and were then subjected to sucrose density gradient centrifugation. HCV RNA sedimented to a density of 1.22 g/ml rather than 1.18 g/ml (Fig. 1C), indicating that the density of HCV particles became higher due to de-envelopment. Transmission electron microscopy (TEM) of the 1.18 g/ml fraction, which was subjected to negative staining after concentration, revealed particle structures with diameters of 30–60 nm and a major particle size of 50 nm (Fig. 1D). No similar particle-like structures were observed in the same density fraction of the RCYM1 monolayer culture (Fig. 1E) or in the 1.23 g/ml fraction of the RCYM1-RFB culture (data not shown). These results indicate that, in the RFB system, the production and secretion of HCV-LPs is possible with a selectable dicistronic HCV genome.

Production and secretion of HCV-LPs from spheroid culture of RCYM1 cells using TGP

In the 3D RFB culture system for RCYM1 cells, extracellular secretion of HCV-LPs was observed. Based on this observation, we hypothesized that morphological changes occurring in 3D culture, such as polarity formation, promote advantageous in the assembly of viral proteins, particle formation, and extracellular secretion. To examine whether similar phenomena could be observed in other 3D culture systems, we investigated HCV-LP expression using a 3D culture system with TGP as a carrier.

TGP is a biocompatible polymer made from conjugates of polyethyleneglycol and poly-*N*-isopropylacrylamide, which is a thermoresponsive polymer composed of *N*-isopropylacrylamide and *n*-butylmethacrylate. The TGP solution possesses sol-gel transition properties; it is water soluble (sol phase) at temperatures below the transition temperature, and it is insoluble (gel phase) above it. It is possible to manipulate the transition temperatures through molecular engineering. The transition temperature for TGP in the present experiments was approximately 20 °C.

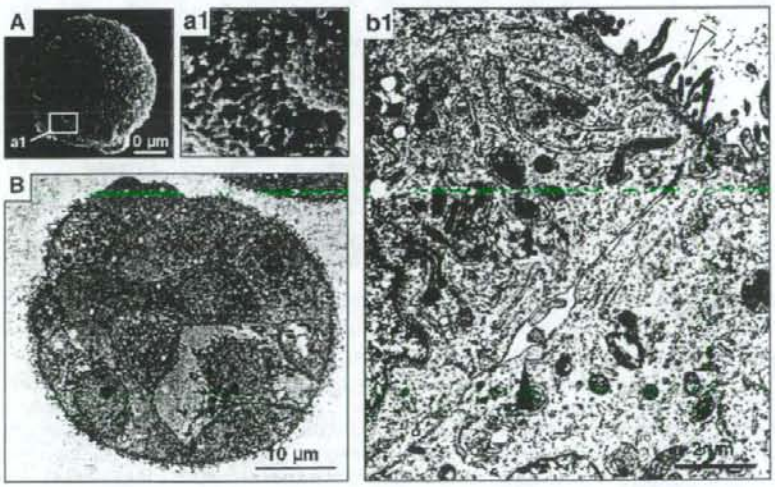

Fig. 2. Huh-7 and RCYM1 cells form spheroids in thermoreversible gelation polymer (TGP). Scanning electron microscopy (A and a1) and transmission electron microscopy (B and b1) of RCYM1 cells cultured in TGP for 8 days. Open arrowhead, microvilli; closed arrowheads, bile canaliculi-like structures.

RCYM1 cells, which were seeded into the TGP, formed three-dimensional compacted aggregates called spheroids after 3 days of culture, and numerous spheroids with diameters of approximately 1 mm were observed after 7–10 days of culture. After 8 days of culture, the spheroids were fixed and examined by scanning electron microscopy (Figs. 2A and a1) and ultrathin sections were examined by TEM (Figs. 2B and b1). Well-developed microvilli, a feature of polarized epithelium, were observed on the cell surface (Figs. 2A and a1). Bile canaliculi-like structures were also observed within intercellular spaces, and they appeared to be connected via tight junctions (Figs. 2B and b1). This cytomorphology, similar to that observed in the RFB culture (Kawada et al., 1998; Matsuura et al., 1998), correlated well with the features of mature liver tissue.

It is known that the replication of HCV replicons in Huh-7 cells depends on host cell growth. We found that the growth of RCYM1 cells in the TGP culture system was significantly slower than that of cells in monolayer culture (Fig. 3A). Accordingly, the expression of HCV proteins (Fig. 3B) in the RCYM1 spheroids was apparently lower compared to those observed in the monolayer cells. The viral RNA copy number in the spheroids was approximately one tenth of that in the monolayer culture (data not shown). The results of sucrose density gradient analysis of culture supernatant demonstrated co-sedimentation of HCV RNAs and core proteins at a density of 1.15–1.20 g/ml, with a peak at 1.18 g/ml (Figs. 3C and D). This distribution was consistent with the pattern obtained in RFB culture (Figs. 1A and B). It should be noted that in these experiments, lower cell numbers were used in the 3D cultures than in the monolayer cultures because of the slower growth of cells. As estimated from the quantitative data of the 1.15–1.20 g/ml fractions of the culture supernatants, 0.1–1 copies of HCV RNA/cell/day are produced and assembled into viral particles in the TGP-cultured RCYM1 cells.

TEM analysis of the 1.18 g/ml fraction after negative staining showed particle structures with a diameter of 50–60 nm and spike-like projections (Fig. 3E). Observation of ultrathin sections indicated a lipid bilayer-like membrane structure with a

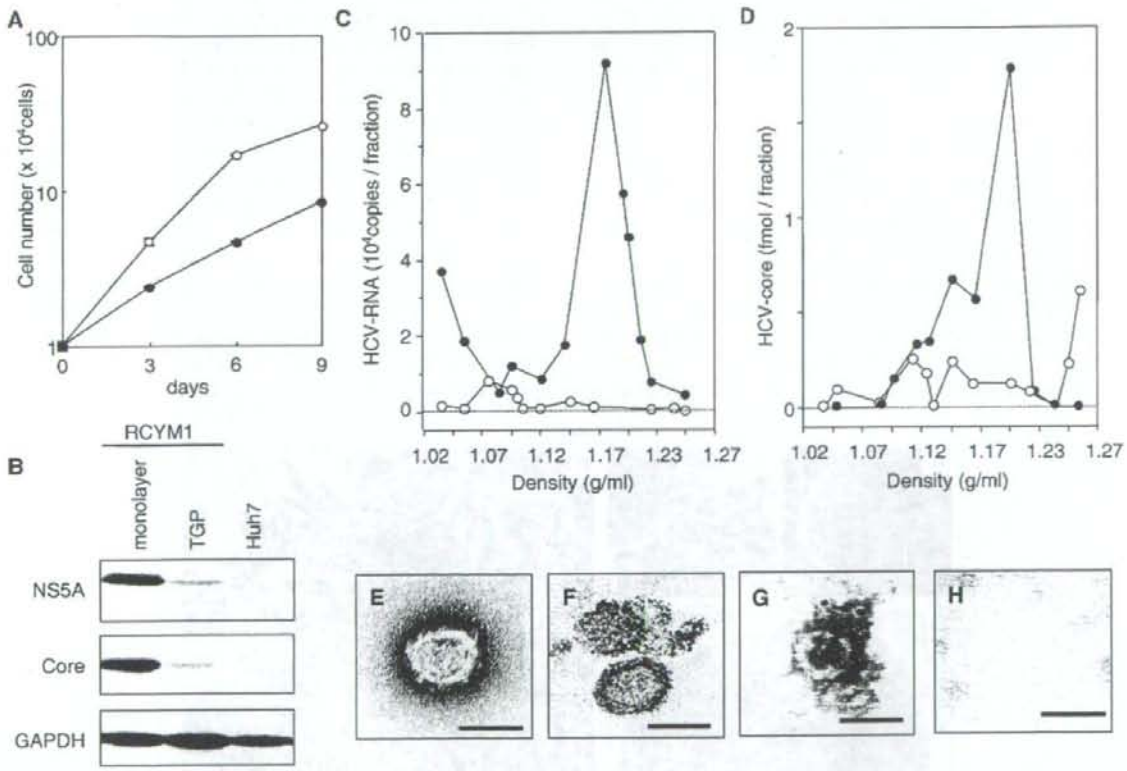

Fig. 3. Expression of HCV proteins in RCYM1 cells and secretion of viral particles in TGP culture. (A) Cell growth curves of the TGP (closed circles) and monolayer (open circles) culture of RCYM1 cells. Cells were harvested at days 0, 3, 6, and 9 postinoculation and cell numbers were determined. (B) Western blotting of HCV core and NS5A proteins in RCYM1 cells and control Huh-7 cells. (C, D) Sucrose density gradient analysis of culture supernatants of RCYM1 cells. The culture supernatants were fractionated as described in Materials and methods. HCV RNA (C) and core protein (D) in each fraction were determined by ELISA and real-time RT-PCR, respectively. Representative data from three independent experiments are shown. Closed circles, TGP culture; open circles, monolayer culture. (E–H) Electron microscopy of HCV-like particles (HCV-LPs) in the supernatants of TGP-cultured RCYM1 cells. (E) Negative staining of HCV-LPs in the 1.18 g/ml density fraction. There was no spherical structure in 1.05 g/ml density fraction, as shown in panel H. (F) Ultrathin section of HCV-LPs. Precipitated HCV-LP samples were prepared from the 1.18 g/ml fraction as described in Materials and methods. (G) Immunogold labeling of HCV-LPs with an anti-E2 antibody in the 1.18 g/ml density fraction. Gold particles, 5 nm; scale bars, 50 nm.

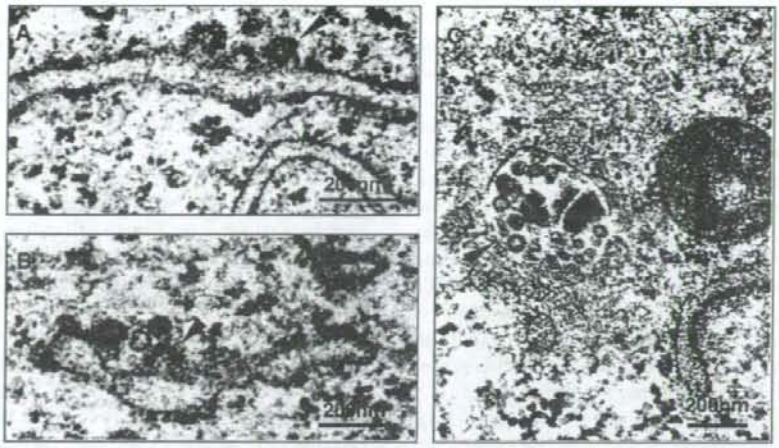

Fig. 4. Electron microscopy of ultrathin sections of RCYM1 cells grown in TGP. HCV-LPs in TGP-cultured RCYM1 cells. Spherical virus-like particles 50–60 nm in diameter (arrowheads) were observed at the ER membranes (A, B) and in the cytoplasmic vesicles (C).

width of approximately 5 nm (Fig. 3F). Immunoelectron microscopic study using anti-E2 antibody revealed HCV envelope protein(s) on the particle surface (Fig. 3G). Substantial amounts of HCV RNA were detected in the 1.03–1.05 g/ml fractions of the supernatant (Fig. 3C); however, HCV-LP structures were not observed in these fractions (Fig. 3H). These results were consistent with those from the RFB system, as shown above. The efficacy of 3D cell culture systems in virion formation was thus demonstrated in both the RFB and TGP culture systems using human liver-derived cells.

Ultrastructural localization of HCV-LPs in TGP-cultured spheroids of RCYM1 cells

We next determined the intracellular localization of HCV-LPs produced in RCYM1-TGP culture at the ultrastructural level by electron microscopic (EM) analysis of ultrathin sections. Spherical particles having membrane-like structures with short surface projections (diameter, 50–60 nm) were observed primarily at the endoplasmic reticulum (ER) membrane (Fig. 4A) as well as in the dilated cisternae of the ER (Fig. 4B). In vesicles, these virus-like particles were frequently associated with amorphous materials (Fig. 4C). In a previous study, Shimizu et al. (1996) report that virus-like particles with similar morphology and size were observed in human B cells infected with HCV. No similar particle-like structures were observed in RCYM1 cells in monolayer culture or in subgenomic replicon 5–15 in cells in TGP culture (data not shown).

In order to determine whether the virus-like particles observed by conventional TEM in the present experiment were HCV-LPs, we conducted immunoelectron microscopic analysis with anti-core antibody and anti-E1 antibody. Double-labeling experiments showed that the virus-like particles associated with the ER membrane exhibited immunoreactivity for both HCV proteins, and that the E1 protein surrounded the core proteins (Fig. 5A). To the best of our knowledge, this is the first report to clearly demonstrate that the viral envelope protein surrounds the core protein in HCV particle formation. As a negative control, thin sections prepared from subgenomic RNA containing 5–15 cells were stained with these antibodies and were found to exhibit negligible levels of background immunostaining (data not shown).

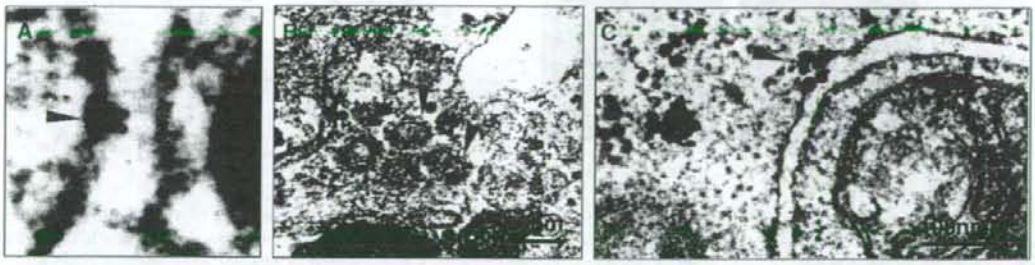

Fig. 5. Immunoelectron microscopy of ultrathin sections of TGP-cultured RCYM1 cells. (A) Double immunostaining with anti-E1 and anti-core monoclonal antibodies. Core protein-specific gold particles (10 nm in diameter) and E1 protein-specific gold particles (5 nm in diameter) formed rosettes on the surface of the ER membrane. (B and C) Silver-intensified immunogold staining with anti-core (B) and anti-E1 (C) antibodies. The second antibody conjugated with gold particles 1.4 nm in diameter was applied, followed by enlargement of the particles by the silver enhancement reagent. Arrowheads indicate virus-like particles reacting with anti-core and/or anti-E1 antibodies.

It is generally difficult to visualize intracellular microstructures and perform antigenic protein localizations using immunogold electron microscopy due to the low resolution and contrast of micrographs. In order to overcome this difficulty, we applied a silver-intensified immunogold labeling method in our experiment (Figs. 5B and C). Using this method, antigen-reactive immunogold particles approximately 20 nm in diameter were observed. Specific immunolabeling of core and E1 protein was detected in the ER or on the ER membranes. Intense immunopositive reactions were also seen on the virus-like particles observed in cytoplasmic vesicles and on ER membranes; however, no such immunolabeling was observed when normal mouse serum was used as a first antibody (data not shown). These results confirm the ultrastructural observations of conventional TEM and suggest that the formation of HCV particles is achieved by budding of the putative core particles at the ER membrane.

Infectivity of HCV-LPs depends on E2 glycoprotein

To determine whether HCV-LPs released from RCYM1 cells cultured in the TGP system are infectious, we inoculated naive Huh-7.5.1 cells (Zhong et al., 2005), which are HCV-negative Huh-7.5 (Blight et al., 2002)-derived cells, with a culture supernatant of RCYM1 spheroids. HCV RNAs in the cells at days 0, 1, 2, 3, and 7 postinoculation were determined by real-time RT-PCR. Fig. 6A shows the kinetics of HCV RNA after the inoculation of HCV-LPs. HCV RNA levels in the infected Huh-7.5.1 cells fluctuated at the indicated times, reaching 10^3–10^4 copies/μg of cellular RNA at days 1–7. Immunofluorescence staining 4 days postinoculation revealed that approximately 1% of cells were positive for NS5A protein (Fig. 6B). In contrast, no NS5A-positive cells were detected when the cell supernatant sample obtained from 5 to 15 cell cultured in TGP was used to inoculate Huh-7.5.1 cells (data not shown). These results suggest that HCV-LPs released from TGP-cultured RCYM1 cells are infectious.

To further determine whether viral envelope proteins mediate infection by HCV-LPs, we preincubated HCV-LPs with the anti-E2 monoclonal antibody AP33, which demonstrates potent neutralization of infectivity against HCV pseudoparticles carrying E1 and E2 proteins representative of the major genotypes 1 through 6 (Owsianka et al., 2005), or with patient sera with high titers of HCV neutralization of binding (NOB) antibodies (Ishii et al., 1998), or with anti-FLAG antibody (Fig. 6C). NOB antibodies have the ability to neutralize the binding of E2 protein to human cells (Rosa et al., 1996), and NOB3 and NOB4 were sera obtained from patients who recovered naturally from chronic hepatitis C (Ishii et al., 1998). Intracellular HCV RNA levels were decreased by 43%, 28%,

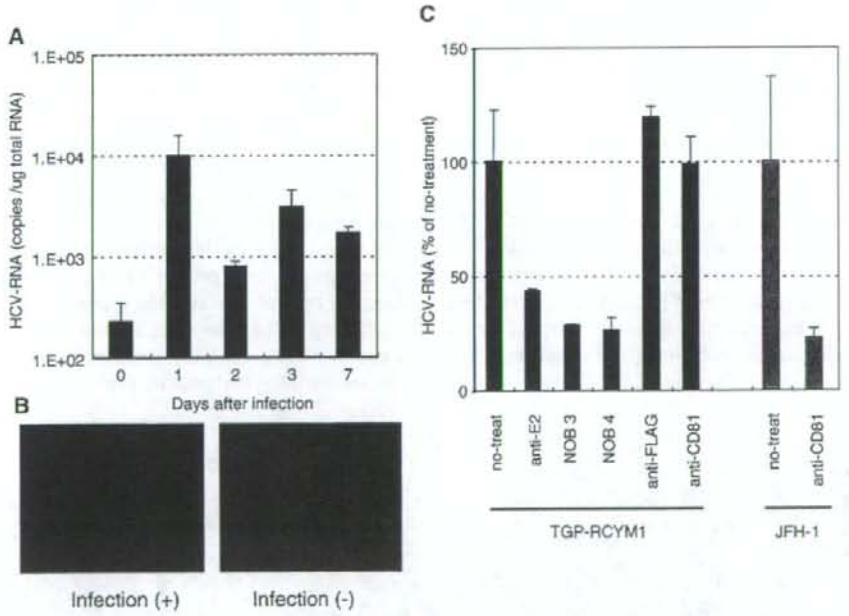

Fig. 6. Infectivity of HCV-LPs secreted from TGP-cultured RCYM1 cells and neutralization of the infection. (A) Kinetics of HCV RNA after the infection of HCV-LPs. Huh-7.5.1 cells were infected with HCV-LPs and harvested at days 0, 1, 2, 3, and 7. HCV RNAs in the cells were determined by real-time RT-PCR. (B) Huh-7.5.1 cells infected with HCV-LPs (upper panel) or without infection (lower panel) were cultured for 4 days, followed by immunostaining with anti-NS5A antibody. Nuclei were counterstained with 4′,6-diamidino-2-phenylindole (DAPI). (C) Huh-7.5.1 cells were infected with HCV-LPs after pretreatment with anti-E2 antibody AP33, neutralization of binding (NOB) antibodies, or anti-FLAG antibody. Anti-human CD81 antibody was preincubated with Huh-7.5.1 cells prior to the infection. Huh-7.5.1 cells were infected with HCV-LPs derived from TGP-cultured RCYM1cells or JFH1 virus and incubated for 4 days; HCV RNAs in the cells were determined by real-time RT-PCR. The inhibition rate is given as the percentage of the no-treatment controls. Average values with standard deviations in triplicate samples are shown. Closed bars, HCV-LPs secreted from TGP-cultured RCYM1 cells; shaded bars, JFH1 virus.

and 26% in the presence of AP33, NOB3, and NOB4, respectively. No reduction of viral RNA in infected cells was observed following treatment with anti-FLAG antibody. Thus, the present results suggest that viral envelope proteins play a crucial role in the infectivity of HCV-LPs produced by RCYM1 cells cultured in TGP. We further tested anti-CD81 antibody for inhibition of the virus infection in our system. As shown in Fig. 6C, pretreatment of the cells with the anti-CD81 antibody resulted in no inhibition of the intracellular HCV RNA level in the infected cells. In contrast, under the same condition of treatment, the antibody efficiently inhibited the infection of JFH-1 virus, which was produced from the HCV JFH-1 molecular clone as previously described (Wakita et al., 2005; Zhong et al., 2005), suggesting that CD81 has no or little, if any, need for the infection of HCV produced in our system.

Potential use of the TGP culture system for HCV production and evaluation of antiviral agents

In a recent report, Lindenbach et al. (2005) found that a cell culture system supporting complete replication of an HCV genotype 2a clone is useful for the evaluation of antiviral drugs. However, to date this complete HCV culture system has not been extended to genotype 1b, which is more frequently detected in patients with hepatitis C and is the most difficult to treat.

We show here the potential utility of the TGP culture of RCYM1 cells for evaluating anti-HCV drugs (Fig. 7). Intracellular HCV RNA levels in TGP-cultured RCYM1 cell spheroids were reduced by 90% after 3 days of culture with 100 IU/ml of IFN-α (Fig. 7A). Likewise, the extracellular HCV particle level, which was calculated using the HCV RNA copy number of the 1.18 g/ml supernatant fraction, was reduced by 89% by IFN-α treatment (Fig. 7B). Moreover, the production of HCV particles was inhibited by treatment with 100 μM RBV to the same degree (85%) as intracellular HCV RNA (Fig. 7B). The level of HCV RNA detected in the 1.04 g/ml fraction of the culture supernatant of the untreated group was approximately one fourteenth of that in the 1.18 g/ml fraction, and the level increased with the addition of IFN-α or RBV (Fig. 7B). Although the mechanism underlying this increase is unknown, a similar phenomenon was observed when several highly cytotoxic agents were evaluated using TGP-RCYM1 cultures (data not shown). It is therefore likely that some cellular proteins associated with HCV RNA are released into the culture supernatant as a result of cell death caused by the moderate cytotoxic effects of IFN and RBV.

Collectively, these results demonstrate that the HCV production model based on TGP culture is useful for evaluating HCV particle production and the inhibitory effects of anti-HCV drugs.

Discussion

In the present report, we describe that HCV-LPs are assembled and released from Huh-7 cells harboring a dicistronic genome-length Con1 HCV RNA in two independent 3D culture systems. The HCV-LPs closely resemble virus-like particles detected in the sera of patients with hepatitis C in terms of both particle size and morphology. The HCV-LPs released into the culture supernatant have a buoyant density of approximately 1.18 g/ml, which is much higher than that of putative HCV particles isolated from patient sera reported previously (Andre et al., 2002; Kanto et al., 1994; Nakajima et al., 1996; Trestard et al., 1998) and slightly higher than the average density of virus particles produced with the JFH-1 isolate (Wakita et al., 2005). One possible explanation is that the HCV particles are highly bound to lipids and low-density lipoproteins in patient sera. In agreement with a recent report (Wakita et al., 2005), our EM examination demonstrated that HCV-LPs are 50–60 nm in diameter and are composed of core-like particles with a diameter of approximately 30 nm that are surrounded by ER-derived E1/

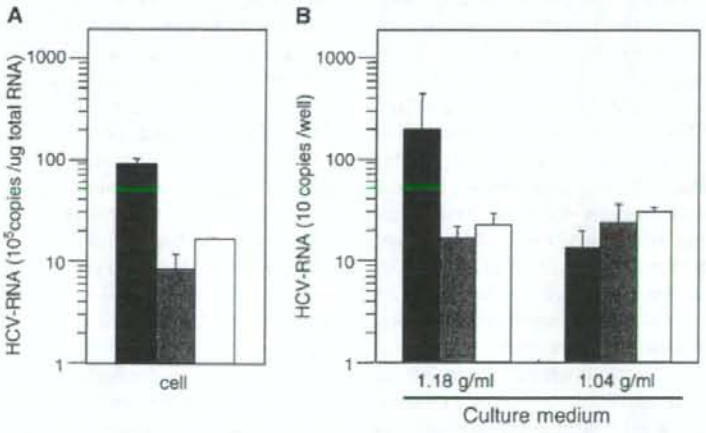

Fig. 7. Inhibition of HCV-LP production by IFN and RBV. TGP-cultured RCYM1 cells were treated with 100 IU/ml IFN-α or 100 μM RBV, and HCV RNAs in the cells (A) and in the culture media (B) were then determined. Culture media from each sample were fractionated by sucrose gradient centrifugation and HCV-LP positive (1.18 g/ml) and negative (1.04 g/ml) fractions were assayed. Average values with standard deviations in triplicate samples are shown. Closed bars, no-treatment control; shaded bars, IFN-α; open bars, RBV.

E2 proteins. These particles are observed at the ER membranes and in dilated cisternae of the ER, suggesting that the interaction of the ER membrane containing HCV envelope proteins with the viral core protein drives the budding process of HCV particles into the ER lumen.

Although studies on the ultrastructure and morphogenesis of HCV-LPs have been conducted using recombinant viral vectors carrying HCV structural protein genes (Baumert et al., 1998; Blanchard et al., 2002, 2003), the present study provides the first visual evidence of assembly and budding of HCV particles in a heterologous expression system in which a full-length viral genome is replicating and the viral particles are secreted into the culture medium. We also demonstrated that the HCV-LPs produced in our 3D culture system are infectious and that their infection is prevented by the monoclonal antibody AP33 directed against E2 (Owsianka et al., 2005) as well as by NOB antibodies (Ishii et al., 1998), which are sera of patients naturally resolving from chronic hepatitis C and exhibiting neutralizing activity. This result is consistent with the recent demonstration that E2 is required for the infectivity of JFH-1 virus (Wakita et al., 2005). It has been shown that CD81 interacts with E2 (Pileri et al., 1998) and that anti-CD81 antibodies or a soluble CD81 fragment block the infection of Huh-7 cells with either pseudotyped retroviral particles, JFH-1 virus or J6/JFH1 chimera (Lindenbach et al., 2005; Netski et al., 2005; Wakita et al., 2005; Zhong et al., 2005). Inconsistent with these studies, however, we found that anti-CD81 antibody did not inhibit the virus infection in our system. Although CD81 is considered to represent an important component in HCV entry, there are several other candidate cellular receptors for HCV (Bartosch and Cosset, 2006) and a study has demonstrated that in vitro binding of HCV to hepatoma cell lines was not inhibited by the anti-CD81 antibody (Sasaki et al., 2003).

In a previous report (Aizaki et al., 2003), we describe the production and release of infectious HCV particles from a human hepatocellular carcinoma-derived cell line, FLC4, using RFB culture in two experiments: inoculation of cells with infectious plasma from an HCV carrier and transfection of cells with viral RNA transcribed from the full-length cDNA of genotype 1a, which is known to infect chimpanzees. These findings prompted us to use the RFB system to create a culture model of HCV production based on genome-length dicistronic viral RNA, which has not been found to produce viral particles in standard monolayer cultures. As expected, HCV-LPs were produced and secreted into the medium during RFB culture of RCYM1 cells, whereas virus production was not observed in the conventional monolayer culture of RCYM1 cells. The presence of the viral envelope protein(s) on the HCV-LPs obtained in the RFB culture was strongly suggested from their density analysis with and without NP40 treatment.

We also created another 3D environment supportive of RCYM1 culture using TGP, a chemically synthesized biocompatible polymer which has a sol-gel transition temperature, thus enabling us to culture cells three-dimensionally in the gel phase at 37 °C and to harvest them in the sol phase at 4 °C, without enzyme digestion (Yoshioka et al., 1994). In contrast to other matrix gels made from conventional natural polymers and developed for 3D culture, including matrigel (Kleinman et al., 1986), collagen gel (Lawler et al., 1983), and soft agar, TGP has several advantages that allow us to investigate the functional characteristics of epithelial cells, their tissue-like morphology, and their potential clinical applications. The use of 3D culture materials other than TGP requires treatment with appropriate digestive enzymes or heating to collect cells grown as spheroids from the culture media, and the matrices may damage the cultured cells to some extent. Thus, it is difficult to keep the viable cells in a functionally and structurally intact. In addition, because matrigel and collagen gel are made from animal or tumor tissue, the possibility that certain pathogens or unidentified factors might influence cell function cannot be excluded. In the present study, we found that Huh-7 and RCYM1 cells formed an organized structure of spheroids after 7–10 days of culture in TGP, and that HCV-LPs were assembled and released from RCYM1 spheroids, as observed in RFB culture. It can be ruled out that HCV-LPs, RNA, and core protein detected in the TGP culture supernatant are released by damaged and/or broken cells because neither digestive enzymes nor heating is used in the culture procedures and no cell damage has been observed in the cultures.

It remains to be clarified why HCV particles were produced from Huh-7 cells harboring the genome-length dicistronic HCV RNA more efficiently in the 3D cultures than in the monolayer cultures. However, this might be related to the fact that directional protein transport in hepatocytes occurs more readily in 3D culture. EM examination demonstrated that, in the RFB and TGP culture systems, human hepatoma cells, such as Huh-7, FLC4, and FLC5 cells, self-assemble into spheroids with possible polarized morphology in which microvilli develop on the cell surface and channels resembling bile canaliculi and junction structures are created in the intercellular spaces (Aizaki et al., 2003; Iwahori et al., 2003). In contrast, human hepatoma cells adhere when grown on a plastic surface, growing as a flat monolayer without exhibiting the characteristics of polarized epithelium. In general, the interaction of viruses with polarized epithelia in the host is one of the key steps in the viral life cycle. A variety of viruses, especially enveloped viruses, mature and bud from distinct membrane domains of the host cells (Compans, 1995; Garoff et al., 1998; Schmitt and Lamb, 2004; Takimoto and Portner, 2004). For example, several respiratory viruses, such as influenza virus, parainfluenza virus, rhinovirus, and respiratory syncytial virus, are released preferentially from the apical surface. Conversely, other viruses egress from the basolateral membrane; these include vesicular stomatitis virus, Semliki Forest virus, vaccinia virus, and certain retroviruses. Thus, it is likely that more organized intracellular trafficking pathways exist in the 3D culture of Huh-7-derived cells, thereby driving the assembly and release of HCV.

The efficient production of HCV in 3D cultures could also be due to the reduction of HCV RNA replication and/or translation in 3D cultures as compared to those in monolayer cultures. RNA replication and/or translation of HCV replicons in Huh-7 cells are highly dependent on host cell growth (Pietschmann et al., 2001). In the present study, we found that the slow growth of spheroids resulted in reduced expression of HCV protein and